Available online at www.sciencedirect.com

SCIENCE DIRECT®

Materials Letters 58 (2004) 2988–2992

materials letters

www.elsevier.com/locate/matlet

Thermal stability and saturation magnetization of a new series of amorphous $Fe_{80-x}Co_xP_{14}B_6$ ($20 \le x \le 40$) alloys

V.I. Tkatch[a,*], S.G. Rassolov[a], V.V. Popov[a], V.Yu. Kameneva[a], O.A. Petrenko[b]

[a] *Physics and Engineering Institute of National Academy of Sciences of Ukraine, Electronic Properties of Solids, R. Luxemburg Str. 72, 83114 Donetsk, Ukraine*

[b] *Department of Physics, University of Warwick, Coventry CV4 7AL, UK*

Received 9 March 2004; received in revised form 14 May 2004; accepted 20 May 2004
Available online 23 June 2004

Abstract

A series of new $Fe_{80-x}Co_xP_{14}B_6$ ($x = 20$, 25, 30, 32, 35, 40) glasses has been prepared by melt-spinning technique. The FeCo-based glasses crystallize via one stage eutectic reaction into a mixture of a-Fe (bcc) solid solution and a b.c.-tetragonal Fe_3P-like phase at temperatures approx. 50 K higher than the $Fe_{80-x}Ni_xP_{14}B_6$ metallic glasses. The compositional dependence of the crystallization temperatures at constant rate heating of the FeCo-based glasses has a minimum at $x = 30$ that correlates well with the values of the apparent activation energy of crystallization derived from the Kissinger analysis. The as-quenched $Fe_{80-x}Co_xP_{14}B_6$ ribbons within the range examined have superior saturation magnetization in comparison with that of the commercial $Fe_{40}Ni_{40}P_{14}B_6$ glass, for example the maximum value of the saturation magnetization M_s estimated from vibrating sample magnetometer measurements is as high as 153 emu/g (about 1.415 T, for a density of 7.42 g/cm^3) for the $Fe_{48}Co_{32}P_{14}B_6$ alloy.

Keywords: Metallic glasses; Thermal stability; Crystallization; Saturation magnetization

1. Introduction

The metallic alloys with nonequilibrium structure (amorphous and nanocrystalline) are competitive with conventional crystalline soft magnetic materials both in terms of enhanced saturation magnetization and low coercive force and have been extensively used for many kinds of magnetic devices [1,2]. Nevertheless, the development of new glass-forming compositions with improved soft magnetic properties and enhanced thermal stability remains an active area of study due to a growing demand for energy-saving and miniature magnetic devices. The requirements for the soft magnetic alloys with nonequilibrium structures produced by melt quenching involve the design of the proper chemical composition which provides not only improved levels of the properties, but also a high glass-forming ability, good casting properties for the alloy which in turn determine the surface quality and uniformity of the melt-spun ribbons, as well as an enhanced thermal stability of both the magnetic properties (the high Curie temperatures, T_C) and amorphous structure (high crystallization temperatures, T_X).

It is known that the highest saturation magnetization has been achieved in FeCo-based amorphous alloys [3], therefore these alloys have attracted increasing interest over the past few years [2,4–6]. It has been recently shown [6] that the replacement of Ni by Co in the well-known metallic glass $Fe_{40}Ni_{40}P_{14}B_6$ leads to an improvement in the magnetic properties (saturation magnetization, M_s, and permeability) and an enhancement in both T_C and T_X. Given that the highest saturation magnetization both in amorphous, nanocrystalline and crystalline materials has been achieved in the FeCo-based alloys with the Fe/Co ratio of about 3:1 [2,3,7], it is expected that a partial substitution of Fe by Co in the $Fe_{40}Co_{40}P_{14}B_6$ amorphous alloy should lead to a further enhancement of M_s.

The aim of this paper is to present the preliminary results of studies of the structure, thermal stability, and saturation magnetization of $Fe_{80-x}Co_xP_{14}B_6$ ($x = 20$, 25, 30, 32, 35, 40) amorphous alloys produced by a melt-spinning process.

* Corresponding author. Tel.: +380-622-557-726; fax: +380-622-510-703.
E-mail address: vit@depm.fti.ac.donetsk.ua (V.I. Tkatch).

0167-577X/$ - see front matter © 2004 Elsevier B.V. All rights reserved.
doi:10.1016/j.matlet.2004.05.023

2. Experimental procedure

Master ingots of alloys with nominal compositions of $Fe_{80-x}Co_xP_{14}B_6$ ($x=20$, 25, 30, 32, 35, 40) were prepared by induction-melting of the mixtures of pure Fe, Co, B and Co_2P in quartz crucibles in an argon atmosphere. Rapidly quenched ribbons were produced by ejecting is ~5 g charges of the molten master alloys from a quartz nozzle onto a rotating copper wheel (diameter 300 mm, surface velocity of about 30 m/s) in air. The melts were heated to approximately 1423 K and ejected by applying an argon gas overpressure of 25–35 kPa. The ductile and uniform as-cast ribbons were typically several meters long, 2 to 8 mm wide, and 20 to 30 μm thick. The ribbons had the smooth surfaces and well-defined edges which implies good casting properties of the melts.

The structure of the as-quenched and crystallized samples was examined by X-ray diffraction using CoKα radiation in a DRON-3M automated diffractometer. The crystallization behavior of amorphous alloys was studied by differential scanning calorimetry (DSC) in a Perkin-Elmer DSC7 under an Ar atmosphere at scan rates in the range 5–40 K/min. The crystallization temperatures T_X were determined from the temperatures of the exothermic peaks in the DSC scans, while the heats of crystallization ΔH_X were estimated from the peak areas. The saturation magnetization in the as-cast ribbons was measured using an Oxford Instruments vibrating sample magnetometer in applied fields of up to 1 T.

3. Results and discussion

The X-ray diffraction patterns of the as-quenched $Fe_{80-x}Co_xP_{14}B_6$ ribbon samples were all quite similar to the example shown in Fig. 1 (curve a) for $Fe_{50}Co_{30}P_{14}B_6$ alloy. The absence of sharp diffraction peaks, as well as the sizes of the coherently scattering domains estimated from the width of the first halo of about 1.5–1.6 nm, are typical for amorphous metallic alloys. The angle position of the first broad peak in the diffraction patterns is found to increase linearly from $2\theta=52.2°$ to 52.6° with increasing Co content ($x=20$ to 40). The observed tendency is in a general agreement with the compositional dependence of the b.c.c. Fe(Co) lattice spacings in crystalline binary iron–cobalt alloys [7].

The amorphous nature of structure of the melt-spun ribbons is also seen from the DSC thermograms shown in Fig. 2. Crystallization of the alloys investigated occurs through a one-stage transformation in a relatively narrow range of temperatures. In addition, it was found that all the DSC traces exhibit a weak endothermic effect due to the glass transition in the temperature range before onset of crystallization. The glass transition temperature T_g for the $Fe_{40}Co_{40}P_{14}B_6$ glass is marked by arrow in the insert on this Fig. 2. The presence of the glass transition in the DSC scans confirms that the cooling rates used in the melt-spinning process ($\geq 1.5\times10^6$ K/s [8]) were sufficiently high to suppress crystallization of the $Fe_{80-x}Co_xP_{14}B_6$ melts.

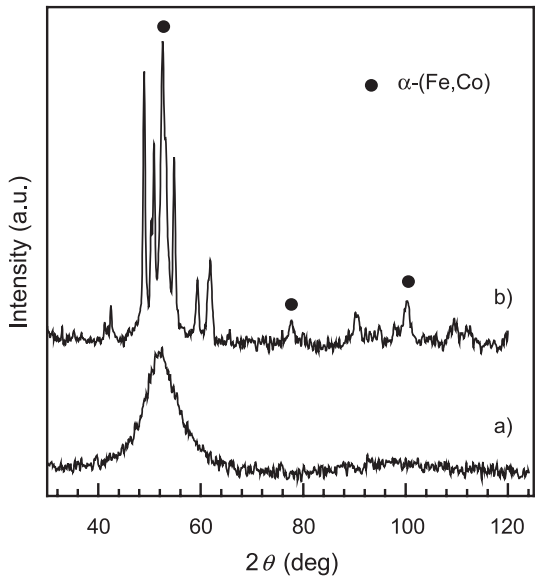

Fig. 1. X-ray diffraction patterns of the melt-spun $Fe_{50}Co_{30}P_{14}B_6$ alloy samples using CoKα radiation: (a) as-prepared; (b) heated above the crystallization peak showing a mixture of a-FeCo solid solution (marked) and the metastable Fe_3P-type phase.

To clarify the crystallization mechanism, analysis of the X-ray diffraction patterns of the specimens heated to temperatures just above the crystallization peaks in the DSC scan was performed. This revealed that the diffraction patterns of all crystallized specimens were quite similar, had no signs of amorphous structure, and consisted of b.c.c. α-(Fe,Co) solid solution and a phase with *d*-spacings close to those of the b.c.t. Fe_3B (Fe_3P-like) phase detected in the crystallized amorphous Fe-B and Fe-Co-B alloys [9]. Given that only one sharp exothermic peak is seen on the DSC curves, the two phase structure of fully crystallized specimens indicate that these $Fe_{80-x}Co_xP_{14}B_6$ amorphous alloys crystallize through eutectic mechanism over the whole compositional range investigated, i.e. simultaneous cooperative formation of two phases. Note that similar crystallization behavior was also seen for the $Fe_{80-x}Ni_xP_{14}B_6$ amorphous alloys [10] and that this is probably typical for $(Fe,Ni,Co)_{80}P_{14}B_6$ glasses.

Based on the DSC curves, the temperatures of the crystallization peaks (T_X) of the $Fe_{80-x}Co_xP_{14}B_6$ glasses were determined and compared in Fig. 3 with the relevant data for $Fe_{80-x}Ni_xP_{14}B_6$ amorphous alloys taken from Ref. [10]. It can be seen from Fig. 3 that the values of T_X of $Fe_{80-x}Co_xP_{14}B_6$ glasses range from 736 to 722 K, vary non-monotonically with the Co content and are approximately 60 K higher that those for their (Fe,Ni) counterparts. If we consider the value of T_X to be a measure of the resistance of the amorphous phase to crystallize, it follows from above that the replacement of Ni by Co results in an enhancement in the thermal stability of the glassy structure over a wide compositional range.

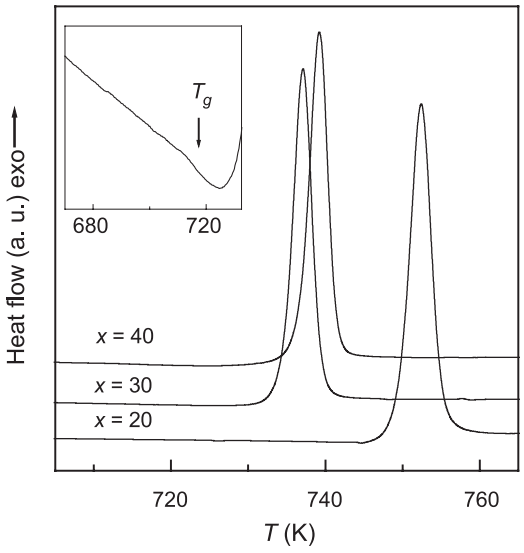

Fig. 2. DSC curves of the as-quenched $Fe_{80-x}Co_xP_{14}B_6$ alloys ($x=20$, 30 and 40) measured at a heating rate of 20 K/min. The glass transition temperature T_g for the $Fe_{40}Co_{40}P_{14}B_6$ amorphous alloy is marked by arrow in the insert.

It is useful to compare the observed compositional variations of T_X for $Fe_{80-x}Co_xP_{14}B_6$ glasses with the values of the activation energy of the crystallization process E_{cr}. The commonly used method for estimating E_{cr} from non-isothermal DSC or DTA data is based on measurements of the shift of it peak temperature with heating rate α (Kissinger technique) [11]. The activation energies determined from the DCS scans at heating rates of 5–40 K/min as slopes of the straight lines of the plots $\ln(\alpha/T_X^2)$ vs. $1/T_X$ for the Fe–Co–P–B glasses investigated are presented in Fig. 4. First of all, it should be noted that these data are in general agreement with the compositional dependence of T_X in Fig. 3. The value of E_{cr} for $Fe_{40}Co_{40}P_{14}B_6$ amorphous alloy is appreciable higher than that for glass $Fe_{40}Ni_{40}P_{14}B_6$ (36500 K [6]). These results indicate that despite a somewhat uncertain physical meaning of such estimated values of the apparent activation energy of crystallization, especially for processes occurring by crystal nucleation and growth [12], the values of E_{cr} may be used as a rough assessment of the relative thermal stability of glasses with similar transformation mechanisms.

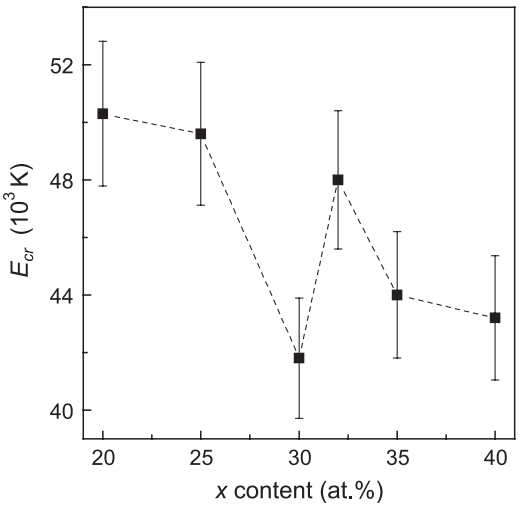

Fig. 4. Changes in the apparent activation energy of the crystallization (E_{cr}) with Co content for the amorphous $Fe_{80-x}Co_xP_{14}B_6$ alloys derived from the Kissinger plots.

All amorphous $Fe_{80-x}Co_xP_{14}B_6$ alloys have soft magnetic properties as it is seen from Fig. 5 where hysteresis M–H loop of the $Fe_{48}Co_{32}P_{14}B_6$ as-prepared ribbon is presented. Fig. 6 shows the saturation magnetization M_s at room temperature as a function of the cobalt content x in amorphous $Fe_{80-x}Co_xP_{14}B_6$ alloys. From this figure, non-monotonic changes of M_s are clearly visible with a maxi-

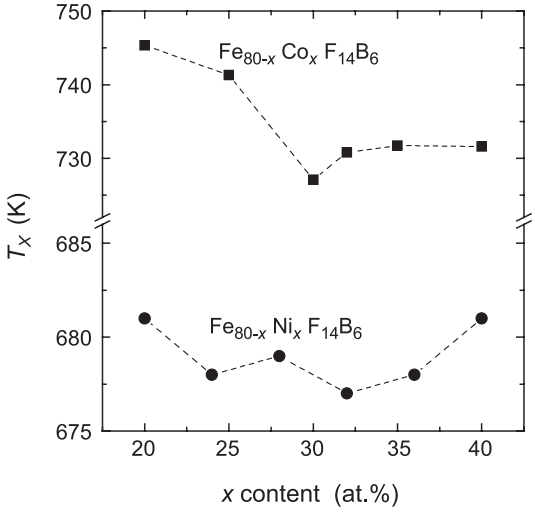

Fig. 3. Changes in the crystallization temperatures (T_X) and heats of crystallization (ΔH_X) estimated from the DSC thermograms at 20 K/min as a function of Co content in $Fe_{80-x}Co_xP_{14}B_6$ alloys.

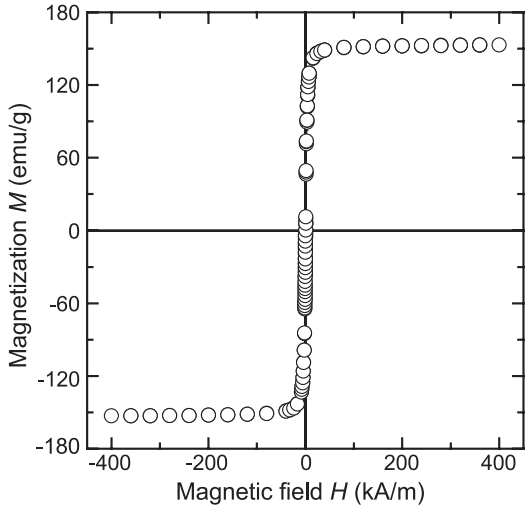

Fig. 5. Hysteresis M–H loop of the as-quenched $Fe_{48}Co_{32}P_{14}B_6$ ribbons recorded by a vibrating sample magnetometer in magnetic field parallel to the ribbon surface.

mum of 153 emu/g at $x=32$ at.% Co. Assuming that the density of the $Fe_{48}Co_{32}P_{14}B_6$ glass to be 7.42 g/mm^3 as for $Fe_{50}Ni_{30}P_{14}B_6$ amorphous alloy [13], this maximum value of M_s corresponds 1.415 T which is significantly higher than 1.04 T reported in Ref. [13] for the latter alloy. Note that an extrapolation of these data to $x=0$ gives the value $M_s \approx 1.35$ T which is close to the 1.36 T found in $Fe_{80}P_{14}B_6$ amorphous alloy [14]. Hence, replacement of Ni by Co in the known series of $(Fe,Ni)_{80}P_{14}B_6$ amorphous alloys results in an improvement of both the saturation magnetization and the thermal stability of glassy structures.

It is noteworthy that the compositional dependence of the saturation magnetization shown in Fig. 6 is similar to that observed in amorphous $(Fe_{1-x}Co_x)_{85}B_{15}$ alloys [3] in which the maximum in the value of M_s was observed at $(Fe_{75}Co_{25})_{85}B_{15}$ composition. The appearance of the maximum of the saturation magnetization, the magnetostriction constant and the first anisotropy constant of Fe–Co–B amorphous alloys vs. Co content was explained by chemical short-range ordering in the amorphous structure. The presence of chemical short-range order in crystalline Fe–Co [15] and amorphous Fe–Co–P–B [16] alloys was deduced by these authors from the changes in the structure of the Mössbauer spectra.

It is known that the first broad peak in the diffraction patterns of liquid and amorphous alloy is a manifestation of short-range atomic correlations in the structure at a length scale of the order of atomic dimensions. Therefore, it may be expected that the changes in the short-range order should influence the width of the amorphous halo. In fact, as can be seen in Fig. 7, the width at half maximum of the first peak B_{HW} varies non-monotonically vs. Co concentration and has a well-pronounced minimum at x ranged between 30 and 35 at.% Co. According to the Scherrer equation, a decreasing B_{HW} implies an increase in the size of the coherently scattering domains which, in turn, indicates an enhancement

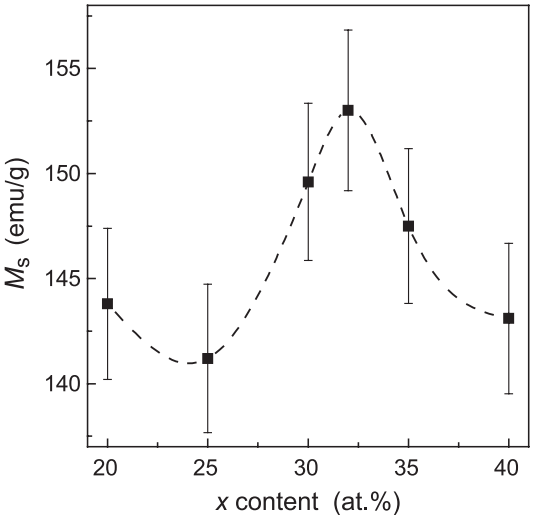

Fig. 6. Compositional dependence of the saturation magnetization at room temperature in the $Fe_{80-x}Co_xP_{14}B_6$ as-prepared amorphous alloys.

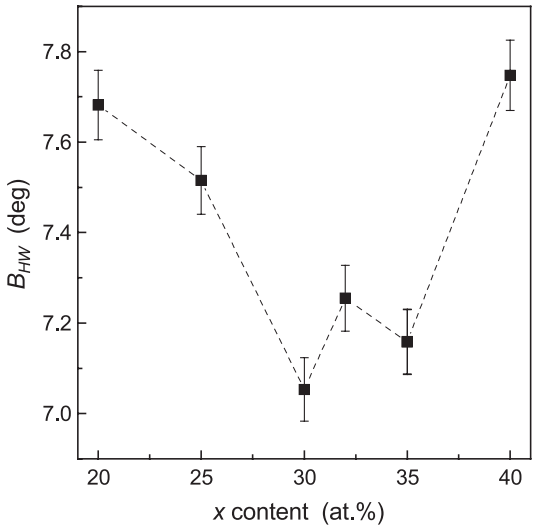

Fig. 7. Variation of the width at half of height of the first peak in the diffraction patterns of the$Fe_{80-x}Co_xP_{14}B_6$ as-quenched amorphous ribbons as a function of Co content.

in the degree of the short-range order within the amorphous structure.

Two possible explanations of chemical short-range order formation in Fe-Co-based alloys were given, namely the selective occupation of the Fe sites by the dilute Co atoms [15] and the repulsion between P and B atoms resulting in two different environments for Co atoms [16]. Taking into account the fact that in certain amorphous alloys (e.g. $Fe_{62.5}Si_{12.5}B_{25}$ [17] and $Fe_{75.5}Si_{13.5}B_7Cu_1Nb_3$ [18]), partial replacement of Fe by Co monotonically lowers M_s, the latter explanation seems preferable. The important role of metalloid atoms in the short-range ordering in Fe–Co-based alloys is apparent in particular in different ratios of Fe and Co atoms at which the maximum in the magnetization saturation properties occurs in the $(Fe,Co)_{80}P_{14}B_6$ (Fig. 6) and $(Fe,Co)_{85}B_{15}$ amorphous alloys [3].

4. Conclusions

In summary, the new amorphous $Fe_{80-x}Co_xP_{14}B_6$ ($20 \le x \le 40$) alloys have been synthesized using a single roller melt-spinning process. The FeCo-based glasses crystallize via a one stage eutectic reaction into a mixture of α-Fe (bcc) solid solution and a b.c. tetragonal Fe_3P-like phase similar to that of the $Fe_{80-x}Ni_xP_{14}B_6$ metallic glasses, but at temperatures approx. 50 K higher than the latter. The compositional dependence of the crystallization temperatures at constant rate heating has minimum at $x=30$ and correlates well with the apparent activation energy of crystallization derived from the Kissinger analysis. The as-quenched $Fe_{80-x}Co_xP_{14}B_6$ ribbons have superior soft magnetic properties compared with those of the well-known $Fe_{40}Ni_{40}P_{14}B_6$ materials. For example, the maximum value of the saturation magnetization M_s estimated from VSM measurements is as

high as 1.415 T for the $Fe_{48}Co_{32}P_{14}B_6$ alloy. The presence of a maximum in the compositional dependence of M_s, is probably due to short-range ordering in the amorphous state which is indicated by a decrease in the width of the first peak in the X-ray diffraction patterns in this compositional range. Given that the soft magnetic properties may be improved by annealing, it is expected that this new series of amorphous alloys is promising for future applications.

Acknowledgements

The authors are grateful to Prof. A.M. Grishin for the provision of laboratory facilities and V.P. Khalievskii for melt-spun ribbons preparation in the Royal Institute of Technology (Stockholm).

References

[1] R. Hasegawa, J. Magn. Magn. Mater. 215–216 (2000) 240.
[2] M.A. Willard, D.E. Laughlin, M.E. McHenry, J. Appl. Phys. 87 (2000) 7091.
[3] L. Kraus, V. Haslar, P. Duhaj, IEEE Trans. Magn. 30 (1994) 530.
[4] J.L. Uriarte, A.R. Yavari, S. Surinach, P. Rizzi, G. Heunen, M. Baricco, M.D. Baro, A. Kvick, J. Magn. Magn. Mater. 254–255 (2003) 532.
[5] I.C. Rho, C.S. Yoon, C.K. Kim, T.Y. Byun, K.S. Hong, J. Non-Cryst. Solids 316 (2003) 289.
[6] V.I. Tkatch, A.M. Grishin, S.I. Khartsev, Mater. Sci. Eng., A Struct. Mater.: Prop. Microstruct. Process. 337 (2002) 187.
[7] R.M. Bozorth, Ferromagnetism, IEEE Press, New York, 1993.
[8] V.I. Tkatch, A.L. Limanovskii, S.N. Denisenko, S.G. Rassolov, Mater. Sci. Eng., A Struct. Mater.: Prop. Microstruct. Process. 323 (2002) 91.
[9] J.L. Walter, S.F. Bartram, I. Mella, Mater. Sci. Eng. 36 (1978) 193.
[10] H. Miura, Sh. Isa, in: S. Steeb, H. Warlimont (Eds.), Rapidly Quenched Metals, North-Holland, Amsterdam, 1985, p. 287.
[11] H.E. Kissinger, J. Res. Natl. Bur. Stand. 57 (1956) 217.
[12] K.F. Kelton, Mater. Sci. Eng., A Struct. Mater.: Prop. Microstruct. Process. 226–228 (1997) 142.
[13] K. Handrich, S. Kobe, Amorphe Ferro-und Ferrimagnetica, Akademic-Verlag, Berlin, 1980.
[14] W. Wolf, JMMM 9 (1978) 200.
[15] I. Vincze, I.A. Campbell, A.J. Meyer, Solid State Commun. 15 (1974) 1495.
[16] J. Durand, D. Aliaga Guerra, P. Panissod, R. Hasegawa, J. Appl. Phys. 50 (1979) 7668.
[17] B.-G. Shen, L. Gao, H.-Q. Guo, J. Appl. Phys. 73 (1993) 5730.
[18] M. Muller, H. Grahl, N. Mattern, U. Kuhn, B. Schell, J. Magn. Magn. Mater. 160 (1996) 284.